

SANDIA REPORT

SAND2013-1960

Unlimited Release

Printed March 2013

Incorporating Supercritical Steam Turbines into Advanced Molten-Salt Power Tower Plants: Feasibility and Performance

James E. Pacheco
Thorsten Wolf
Nishant Muley

Prepared by
Sandia National Laboratories
Albuquerque, New Mexico 87185 and Livermore, California 94550

Sandia National Laboratories is a multi-program laboratory managed and operated by Sandia Corporation, a wholly owned subsidiary of Lockheed Martin Corporation, for the U.S. Department of Energy's National Nuclear Security Administration under contract DE-AC04-94AL85000.

Approved for public release; further dissemination unlimited.



Sandia National Laboratories

Issued by Sandia National Laboratories, operated for the United States Department of Energy by Sandia Corporation.

NOTICE: This report was prepared as an account of work sponsored by an agency of the United States Government. Neither the United States Government, nor any agency thereof, nor any of their employees, nor any of their contractors, subcontractors, or their employees, make any warranty, express or implied, or assume any legal liability or responsibility for the accuracy, completeness, or usefulness of any information, apparatus, product, or process disclosed, or represent that its use would not infringe privately owned rights. Reference herein to any specific commercial product, process, or service by trade name, trademark, manufacturer, or otherwise, does not necessarily constitute or imply its endorsement, recommendation, or favoring by the United States Government, any agency thereof, or any of their contractors or subcontractors. The views and opinions expressed herein do not necessarily state or reflect those of the United States Government, any agency thereof, or any of their contractors.

Printed in the United States of America. This report has been reproduced directly from the best available copy.

Available to DOE and DOE contractors from
U.S. Department of Energy
Office of Scientific and Technical Information
P.O. Box 62
Oak Ridge, TN 37831

Telephone: (865) 576-8401
Facsimile: (865) 576-5728
E-Mail: reports@adonis.osti.gov
Online ordering: <http://www.osti.gov/bridge>

Available to the public from
U.S. Department of Commerce
National Technical Information Service
5285 Port Royal Rd.
Springfield, VA 22161

Telephone: (800) 553-6847
Facsimile: (703) 605-6900
E-Mail: orders@ntis.fedworld.gov
Online order: <http://www.ntis.gov/help/ordermethods.asp?loc=7-4-0#online>



Incorporating Supercritical Steam Turbines into Molten-Salt Power Tower Plants: Feasibility and Performance

James E. Pacheco
Active Response and Denial Department
Sandia National Laboratories
P.O. Box 5800
Albuquerque, NM 87185-0783

Thorsten Wolf and Nishant Muley
Fossil Power Generation
Siemens Energy, Inc.
Orlando, FL 32826

Abstract

Sandia National Laboratories and Siemens Energy, Inc., examined 14 different subcritical and supercritical steam cycles to determine if it is feasible to configure a molten-salt supercritical steam plant that has a capacity in the range of 150 to 200 MWe. The effects of main steam pressure and temperature, final feedwater temperature, and hot salt and cold salt return temperatures were determined on gross and half-net efficiencies. The main steam pressures ranged from 120 bar-a (subcritical) to 260 bar-a (supercritical). Hot salt temperatures of 566 and 600°C were evaluated, which resulted in main steam temperatures of 553 and 580°C, respectively. Also, the effects of final feedwater temperature (between 260 and 320°C) were evaluated, which impacted the cold salt return temperature. The annual energy production and levelized cost of energy (LCOE) were calculated using the System Advisory Model on 165 MWe subcritical plants (baseline and advanced) and the most promising supercritical plants. It was concluded that the supercritical steam plants produced more annual energy than the baseline subcritical steam plant for the same-size heliostat field, receiver, and thermal storage system. Two supercritical steam plants had the highest annual performance and had nearly the same LCOE. Both operated at 230 bar-a main steam pressure. One was designed for a hot salt temperature of 600°C and the other 565°C. The LCOEs for these plants were about 10% lower than the baseline subcritical plant operating at 120 bar-a main steam pressure and a hot salt temperature of 565°C. Based on the results of this study, it appears economically and technically feasible to incorporate supercritical steam turbines in molten-salt power tower plants.

ACKNOWLEDGMENTS

We would like to thank Greg Kolb for his support of this study, his insights, and his inspiration to pursue systems, which yield higher efficiencies in molten-salt power tower plants.

CONTENTS

1. Introduction.....	9
1.1. Current-Technology Molten-Salt Power Tower Plants	10
1.2 Advanced Molten-Salt Power Tower Plants.....	11
1.3 Objectives	13
2. Analysis	15
2.1 Plant Definition.....	15
2.2 Supercritical Steam Turbine Description.....	15
2.3 Once-Through Steam Generator Description	16
2.4 Analysis of Power Block Performance	19
2.5 Trade Studies	20
2.5.1 Impact of Final Feedwater Temperature	20
2.5.2 Impact of Main Steam Pressure.....	21
2.5.3 Half-net Cycle Efficiency.....	22
2.5.4 Salt Return Temperature	23
2.6 Impacts on Receiver, Thermal Storage System, and Power Block Costs.....	23
2.7 Solar Plant Annual Performance and Levelized Cost of Energy	25
3. Conclusions.....	33
4. References	35

FIGURES

Figure 1. The 10 MWe Solar Two molten-salt power tower plant.....	9
Figure 2. Schematic of molten-salt power tower plant.....	11
Figure 3. Model of an industrial supercritical steam turbine based on the Siemens SST-900 steam turbine	16
Figure 4. 3D model view of once-through (BENSON® technology) boiler	17
Figure 5. Schematic of CSP BENSON® steam generator	18
Figure 6. Impact of final feedwater temperature on power block efficiency.....	21
Figure 7. Impact of main steam pressure on power block gross efficiency.....	22
Figure 8. Impact of main steam pressure on half-net cycle efficiency	23

TABLES

Table 1. Plant configurations and variables	15
Table 2. Impact of key thermodynamic parameters (inlet pressure, inlet temperature, and final feedwater temperature) on power block efficiency	19
Table 3. Cold and hot salt pump parasitic power consumption for selected cycles	24
Table 4. Thermal storage system specific costs for selected cycles	25
Table 5. Plant configurations evaluated for annual performance	25

Table 6. Financial assumption used in annual simulations.....	26
Table 7. Tower system costs.....	27
Table 8. Heliostat field.....	28
Table 9. Tower and receiver characteristics	28
Table 10. Power cycle parameters	29
Table 11. Thermal storage parameters.....	29
Table 12. Parasitics parameters.....	30
Table 13. Balance of plant parasitic parameters	30
Table 14. Summary of annual energy production and levelized cost of energy.....	31

NOMENCLATURE

ASME	American Society of Mechanical Engineers
bar-a	bar, absolute pressure
CO ₂	carbon dioxide
CSP	concentrating solar power
DOE	Department of Energy
DSCR	debt service coverage ratio
EPC	Engineering, Procurement, and Construction
FFWT	final feedwater temperature
GWh	gigawatt-hour
HTF	heat transfer fluid
ITD	initial temperature difference
IRR	internal rate of return
kg	kilogram
kJ	kilojoule
kW	kilowatt
kWe	kilowatt electric
kWh	kilowatt hour
LCOE	levelized cost of energy
LHV	lower heating value
m	meter
MACRS	modified accelerated cost recovery system
mm	millimeter
MST	main steam temperature
MW	megawatt
MWe	megawatt electric
MWh	megawatt hour
MWht	megawatt hour thermal
MWt	megawatt thermal
OD	outer diameter
PPA	power purchase agreement
psia	pounds per square inch absolute
rad	radian
s	second
SAM	System Advisory Model
TES	thermal energy storage
SNL	Sandia National Laboratories
TIOs	technology improvement opportunities
TMY2	typical meteorological year 2
TSS	thermal storage system
Wac	watts alternating current
Wt	watts thermal

Intentionally left blank.

1. INTRODUCTION

Molten-salt power tower technology has been developed over three decades in the United States (US) and Europe. The basic research has been conducted at many institutes across the world including Sandia National Laboratories (SNL) in Albuquerque, New Mexico; the Centro de Investigaciones Energéticas, Medioambientales y Tecnológicas (CIEMAT) in Almería, Spain; and the THEMIS facility in Cerdanya, France. As part of this research, many component- and system-level advances were made on receivers, thermal storage, and steam generator designs. These developments led to the demonstration of a full molten-salt power tower plant with integrated components called Solar Two.

The Solar Two plant, a 10 MWe system deployed in California, replaced the Solar One steam receiver and rock/oil thermocline with a molten-salt receiver, two-tank molten-salt thermal storage system, and steam generator, reusing the heliostat field, tower, and steam turbine (Figure 1). Solar Two operated from 1996 to 1999. The most significant attribute demonstrated at Solar Two was its ability to dispatch solar-generated, grid-connected electrical power independent of solar collection. This feature enabled solar power tower plants to compete with dispatchable technologies without fossil-fuel backup. The thermal storage system provided an inherent advantage over solar plants without storage (e.g., direct steam power tower plants or photovoltaic plants). Results showed that solar energy could be stored effectively in the molten-salt thermal storage system to generate electricity during cloudy weather, after sunset, or through the night with daily thermal efficiencies greater than 98%. In one demonstration of dispatchability, Solar Two produced grid-connected power continuously for 154 hours. Tests successfully demonstrated that the receiver system, thermal storage system, steam generator/electric power generation systems, and auxiliary loads met their peak efficiencies goals [1].



Figure 1. The 10 MWe Solar Two molten-salt power tower plant

As a result of research and demonstrations, the first commercial molten-salt power tower plants are now online or under construction. The Gemasolar 19.9 MWe plant located in Andalucía, Spain, came online in 2011. It has a 15-hour thermal storage system designed to provide 65% capacity factor from solar or 75% when supplemented with fossil fuel. In the US, SolarReserve's Crescent Dunes 110 MWe molten-salt power tower plant under construction near Tonopah, Nevada, will have 10 hours of storage and a 50% capacity factor. It is expected to come online late in 2013. These plants use a near-eutectic mixture of sodium nitrate and potassium nitrate as the storage media in a two-tank thermal storage system. Heat is transferred through a steam generator to produce high-pressure supercritical steam, which powers a Rankine-cycle steam turbine.

In an effort to reduce the levelized cost of energy (LCOE) of concentrating solar power (CSP) plants, Sandia National Laboratories and the US Department of Energy (DOE) are exploring more efficient thermodynamic cycles as part of the SunShot Initiative [2]. One key goal of the SunShot Initiative is to reduce the LCOE of CSP plants to 6 cents/kWh by 2020. By increasing the gross cycle efficiency (conversion of heat to electricity), the size of the solar field can be reduced, which reduces the LCOE.

One possibility for increasing the gross cycle efficiency is integrating supercritical steam turbines into power towers. The typical size of supercritical steam turbines used in coal power plants is 400 MWe or larger. For a baseload (70% capacity factor) molten-salt power tower, the turbine size can be up to 160 MWe; its limitation is due to the maximum practical size of the heliostat field and receiver (rated at approximately 1000 MWt). Most of the energy collected during a typical day is stored in a thermal storage tank and dispatched throughout the day and night. In the summer, the turbine operates 24 hours a day.

1.1. Current-Technology Molten-Salt Power Tower Plants

In a current state-of-technology molten-salt power tower plant, cold salt at 290°C is pumped from a cold tank through the receiver located at the top of the tower. Sunlight is reflected from a field of tracking heliostats and concentrated onto the receiver, which heats up the molten salt to 565°C; then the molten salt flows back down to grade level and is stored in a hot tank. To make electricity, hot salt is pumped from the hot tank through a steam generator to make high-pressure (supercritical) superheated steam, and then it is returned to the cold tank. The steam powers a conventional Rankine turbine generator. The molten-salt storage system enables electricity to be produced during the day, through clouds, and at night, independent of solar collection. A schematic of such a plant is shown in Figure 2.

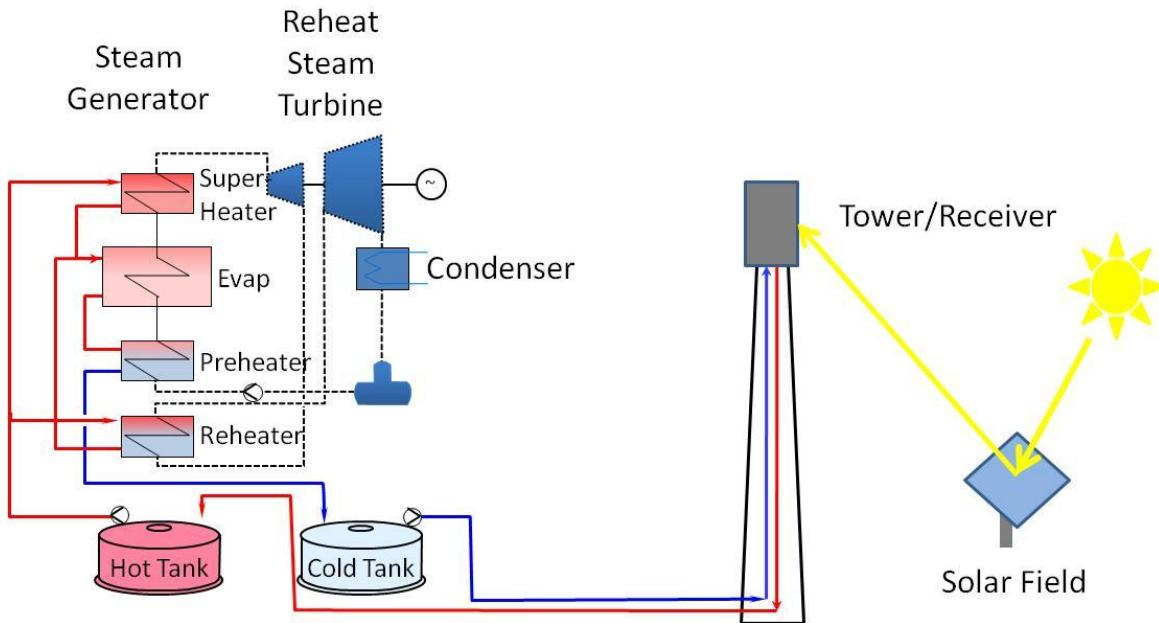


Figure 2. Schematic of molten-salt power tower plant

In the current-technology plant, the main steam pressure is limited to subcritical conditions, typically around 120 bar-a, and the main steam temperature is limited to around 540°C. The plants are designed for subcritical pressures primarily because molten-salt technology was developed around conventional power plant technology. The hot salt temperature at the outlet of the receiver (565°C) limits the maximum live steam temperature. The gross cycle efficiency of the current subcritical technology is approximately 43.0% with wet cooling or 41.2% with air-cooled condensers [3]. The technical risks are too high to deploy advanced, undemonstrated supercritical configurations in the first commercial molten-salt power plants.

1.2 Advanced Molten-Salt Power Tower Plants

A number of advancements were proposed in a power tower technology roadmap, which can reduce the LCOE relative to current-technology power plants [4]. Technology improvement opportunities (TIOs) associated with power tower subsystems were identified in four categories: solar collector field, solar receiver, thermal energy storage, and power block/balance of plant. The power block TIOs identified included the following:

- Advanced power cycle (supercritical steam Rankine, high-temperature air Brayton, and supercritical CO₂ Brayton)
- Parasitic power reduction (receiver pumps, head recovery options, reduction of plant-wide parasitics)
- Hybridization (augmentation with solar to existing fossil power plants or fossil backup of solar plants)

- Dry cooling (reduce water consumption relative to wet cooling)
- Designs for rapid temperature change (respond faster to cloud transients, particularly for direct steam receiver plants)

Of the proposed power block TIOs, advanced power cycles offer the greatest potential reduction in LCOE, with as much as 2 cents/kWh reduction for either supercritical steam or supercritical CO₂ cycles. Development of a power tower plant that implements supercritical steam has less perceived technical risk and is more likely to be adopted by companies deploying power tower technology today because supercritical steam turbines are mature and operating in plants around the world. Not nearly as much technology development is required to implement supercritical steam into a power tower plant as is required to develop an entirely new power cycle, compatible thermal storage, and heat exchangers.

In another study, possible next-generation high-temperature molten-salt power tower plants were explored to determine if there is significant economic benefit to developing molten-salt plants that operate at a higher receiver outlet temperature [3]. Higher temperatures would allow the use of supercritical steam cycles that improve efficiency relative to today's subcritical cycle (~50% versus ~42%). The LCOE of a 565°C subcritical baseline plant was compared with possible future-generation plants that operate at 600 or 650°C. The analysis suggested that ~8% reduction in LCOE could be expected by raising salt temperature to 650°C. However, most of that benefit could be achieved by raising the temperature to only 600°C.

All the subcritical and supercritical plants investigated in [3] were composed of a 1000 MWt receiver, 15 hours of storage (5000 MWht), and a steam power block with a nominal rating between 140 and 165 MWe. Not all the technologies needed to build a plant of this type currently exist. For example, the world's largest molten-salt power tower now under construction in Nevada consists of a 585 MWt receiver and a 2900 MWht thermal storage system. Thus, the receiver/storage technologies studied in [3] are 1.7 times larger than today's technology. Subcritical steam power blocks with an output of 150 MWe currently exist. However, the smallest supercritical power blocks available today are 400 MWe. Thus, the supercritical power blocks studied here are about one-third the size of today's technology.

Because it may not be practical to thermally cycle a supercritical power block daily, it will need to operate nearly 24 hours a day, every day, much like a coal plant operates. This is because the much higher steam pressures (≥ 230 bar-a supercritical versus 125 bar-a subcritical) will result in very thick pipe walls and turbine casings, which increase startup time relative to a subcritical plant.

The bulk hot salt temperature is 565°C in the hot thermal storage tank for current molten-salt power tower technology. Advanced molten-salt receivers were proposed to achieve higher temperatures (up to 600°C) by using nickel alloys for the receiver tube materials [3]. There is a limit to the upper temperature of nitrate salts, which irreversibly decompose above ~620°C. The return cold salt temperature (from the steam generator) is another variable with which to optimize the power block efficiency.

Even though the previous study showed potential cost advantages to developing high-temperature molten-salt plants, the current concern of this report is whether it is feasible to deploy a supercritical steam turbine in the size amenable to molten-salt power towers (100 to 200 MWe) or how difficult is it to convert an existing turbine to supercritical conditions. A smaller supercritical turbine may suffer reduced efficiency due to end losses in the blades of the high-pressure section of the turbine.

1.3 Objectives

The major objectives of this effort are listed below:

1. Define the feasibility of modifying subcritical steam turbines to achieve supercritical conditions at 165 MWe capacities. Define other challenges associated with integrating a supercritical turbine with molten-salt technology, such as development of once-through supercritical steam generators and daily startup and shut down of the power block.
2. Determine the impact on gross cycle efficiency and half-net efficiency of a 165 MWe supercritical steam turbine. Consider effects of pressure, steam temperature (~545 to 580°C), and final feedwater temperature to the molten-salt steam generator (~290 to 320°C).
3. Estimate the cost differential between a 165 MWe supercritical steam turbine power block and a subcritical power block of the same size.
4. Determine the impact of higher hot salt temperatures and cold salt return temperatures on the thermal storage and receiver system costs.
5. Quantify the annual performance and LCOE of a baseline plant and supercritical cycle plants.

Intentionally left blank.

2. ANALYSIS

2.1 Plant Definition

The plant configurations, which we are interested in studying, are defined in Table 1.

Table 1. Plant configurations and variables

Configuration	Molten-salt power tower with two-tank thermal storage
Power block output, gross, MWe	165
Type of cooling	Air-cooled condenser (0.152 bar-a back pressure at 35°C)
Hot salt temperature, °C	566, 600
Cold salt temperature, °C	296, 300, 311, 314, 331
Live steam pressure, bar-a	120 (subcritical) and 230 & 260 (supercritical)
Live steam temperature, °C	553, 580
Final feedwater temperature, °C	260, 290, 320

2.2 Supercritical Steam Turbine Description

Sandia National Laboratories and Siemens teamed together to study the performance, implications, design, and cost of supercritical molten-salt power tower plants. Supercritical steam turbines are common in coal-fired power plants with high power output. Supercritical pressure is associated with low specific volume of steam and hence leads to a very narrow steam blade path at the turbine inlet with relative high secondary losses. For this reason, supercritical steam parameters in full-speed utility type turbines are common only for power output range beyond 500 MW.

As a part of this study, Siemens recommended upgrading a high-speed geared steam turbine from its industrial fleet to supercritical inlet pressure to overcome the limitation described above. The compact size of the high-speed high-pressure turbine reduces losses of the blade path and makes use of the thermodynamic advantage of supercritical steam parameters for an output range of 140 to 200 MW.

The Siemens SST-900 (shown in Figure 3) is an excellent match for the required conditions. It is a dual-casing steam turbine with up to 200 MW power output. It is specifically designed for power-generation applications. To make the best use of the large change in volumetric flow from inlet to outlet, this turbine's steam expansion is divided into two different modules: one high-pressure (HP) turbine and one intermediate-pressure (IP) turbine, operating at different speeds. Optimum performance is ensured by choosing dimensions for each cylinder appropriate to volumetric flow and by using two different and optimized speeds for the HP and LP turbines. With a symmetrical barrel-type HP casing and small dimensions of the hot parts resulting in low thermal and mechanical inertia, this turbine can accept short startup times and rapid load changes.

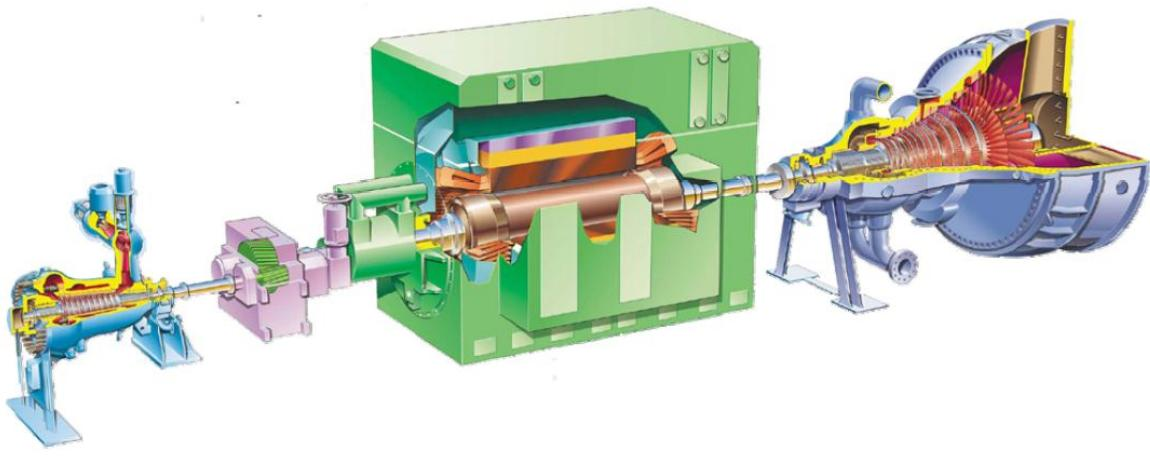


Figure 3. Model of an industrial supercritical steam turbine based on the Siemens SST-900 steam turbine

The development of supercritical steam turbines at Siemens for output up to 200 MW is based on subcritical technology, which has been implemented in CSP plants globally. This type of steam turbine, although requiring a thicker casing due to higher inlet pressure, is well suited for solar applications because of its capabilities for daily cycling, short startup times, and rapid load changes. This turbine has state-of-the-art sealing technology adapted for larger pressure difference, a customized blade design specific to the application, and excellent turbine efficiency.

2.3 Once-Through Steam Generator Description

In current-technology molten-salt power plants, the steam generator consists of four heat exchangers: a preheat to heat subcooled feedwater to slightly below the boiling point, an evaporator and steam drum to boil the feedwater and separate moisture from the steam, a superheater to heat the dry steam to superheated conditions, and a reheater to reheat steam exiting the high-pressure turbine.

However, for supercritical steam conditions, the steam pressure exceeds the critical pressure of water; thus, boiler technology using gravity to separate water and steam is not suitable. Therefore, the kettle-type or drum-type boilers commonly used in CSP plants need to be replaced by steam generators working according to the once-through principle. Siemens has developed a once-through-technology steam generator based on molten nitrate salt as a heating medium that can produce steam at supercritical pressure. Siemens acquired the BENSON® technology in the 1920s, and has made significant leaps in advancing this technology for various applications.

The once-through design (BENSON® technology) makes it possible to integrate the economizer (preheater), the evaporator, and the superheater into a single pressure vessel (Figure 4). This design provides for simplified field assembly compared with current designs for CSP plants with three separate pressure vessels. The need for both salt and water/steam interconnect pipework

between the vessels is also eliminated. Each steam generator consists of a cylindrical shell and two elliptical ends welded to the cylindrical section. Inside the pressure vessel shell the heating surface is installed enclosed by a square metal duct. In between the evaporator and superheater sections of the once-through steam generator a separator system is installed for startup purposes to separate the water from the steam (Figure 5).



Figure 4. 3D model view of once-through (BENSON® technology) boiler

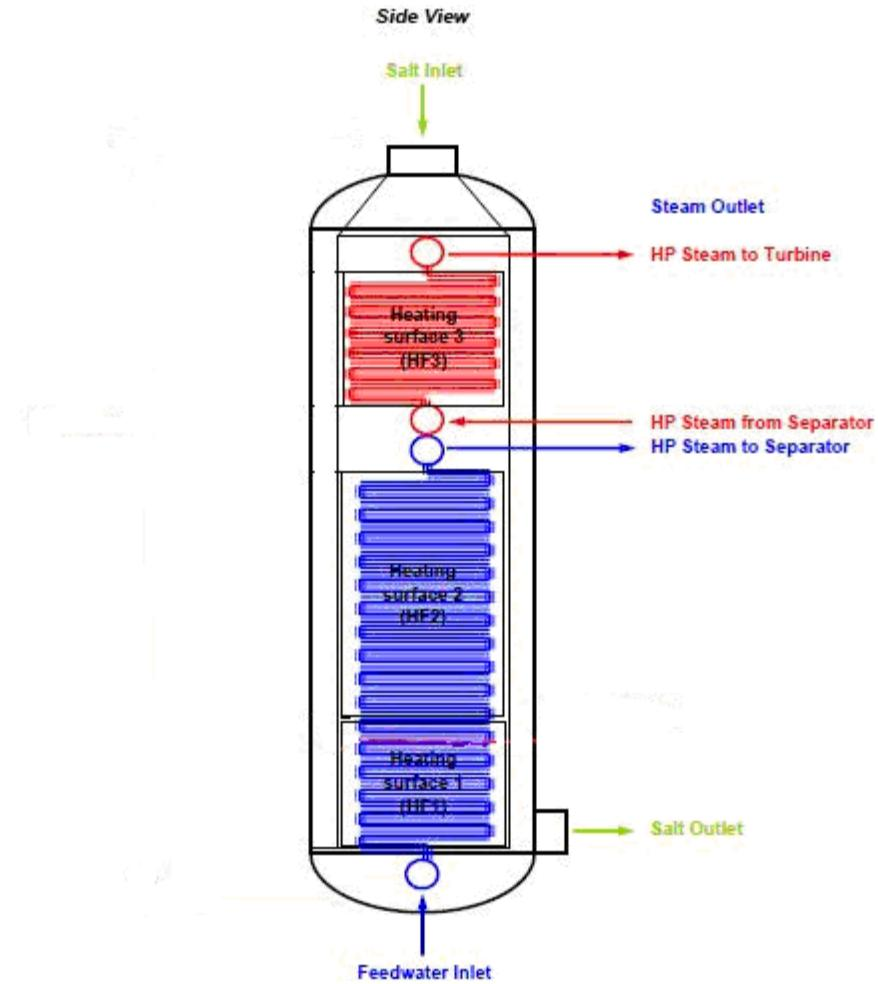


Figure 5. Schematic of CSP BENSON® steam generator

The steam generator is a header-type design, a well-proven technology used worldwide for steam generators and heat exchangers for condensate and feedwater heating. The main advantage of this construction is the high thermal flexibility compared with thick tube sheet constructions (kettle-type boilers).

Molten salt, which is heated up in the solar tower and pumped from the hot salt tank, is used as the heat transfer medium in the once-through steam generators and is supplied via salt pipe to the top of the steam generator. Inside the pressure vessel, the salt is cooled down on the shell side of the pressure vessel and returned via piping to the cold salt tank. The feedwater supplied via pipe from the final HP heater is supplied to the feedwater inlet header arranged at the lower section of the pressure vessel. From this header the feedwater is distributed to the individual parallel tubes. The heating surface design is of the cross-counter-flow type. In the individual tubes the feedwater is preheated, evaporated, and superheated in a once-through mode. The steam produced in the steam generators is collected in the main steam outlet header and fed to the steam turbine via the main steam line. The once-through steam generators are designed for a

vertical installation. The steam generators are installed outdoors and insulated accordingly. All components are designed for outdoor installation. The once-through steam generator is designed, manufactured, and stamped as an ASME Section VIII pressure vessel.

Siemens has also completed the development of a molten-salt steam reheater based on the same header-type design technology of the BENSON® steam generator. The high thermal flexibility of the header type used in the BENSON® steam generator and reheater makes it ideal for a CSP application that requires a daily startup and shutdown and rapid load changes.

However, supercritical steam pressure results in a thick wall in the live steam headers which is sensitive to rapid temperature changes. To avoid high thermal stresses caused by temperature changes during startup, Siemens recommends that the supercritical power block be operated at night at a minimum load of 20 to 25% to reduce the number of starts and decrease the impact on the lifetime of the equipment. A molten-salt power tower with high-capacity factors will minimize the daily startups and cycling.

2.4 Analysis of Power Block Performance

An analysis was conducted on the impact of the thermodynamic parameters described in Table 1 on power block efficiency. The results are summarized in Table 2 for 14 thermodynamic cycles.

Table 2. Impact of key thermodynamic parameters (inlet pressure, inlet temperature, and final feedwater temperature) on power block efficiency

			Cycle													
	Parameter Description	Units	1	2	3	4	5	6	7	8	9	10	11	12	13	14
A	Main Steam Pressure	bar-a	120	120	230	230	230	230	230	230	260	260	260	260	260	260
B	Main Steam Temperature	°C	553	553	553	580	553	580	553	580	553	580	553	580	553	580
C	Cold Reheat Pressure	bar-a	35	35	35	35	35	35	35	35	35	35	35	35	35	35
D	Cold Reheat Temperature	°C	370.7	370.8	285.1	303.2	284.8	302.9	282.5	303	269.3	287.6	269.1	287.2	267	287.2
	Reheat Pressure Drop	%	8%	8%	8%	8%	8%	8%	8%	8%	8%	8%	8%	8%	8%	8%
E	Reheat Steam Pressure	bar-a	32.2	32.2	32.2	32.2	32.2	32.2	32.2	32.2	32.2	32.2	32.2	32.2	32.2	32.2
F	Reheat Steam Temperature	°C	553	553	553	580	553	580	553	580	553	580	553	580	553	580
G	Final Feedwater Temperature	°C	260.8	290.9	260.3	262.9	290	292.1	321.2	321.5	260	262.8	290	292.1	321.2	321.4
H	ACC Back Pressure	bar-a	0.152	0.152	0.152	0.152	0.152	0.152	0.152	0.152	0.152	0.152	0.152	0.152	0.152	0.152
	Gross Power Output	MW	165	165	165	165	165	165	165	165	165	165	165	165	165	165
	Gross Cycle Efficiency	-	0.432	0.432	0.452	0.459	0.455	0.462	0.455	0.462	0.454	0.461	0.458	0.464	0.459	0.465
	Gross Cycle Delta Efficiency	%	base	0.07%	4.59%	6.23%	5.26%	6.83%	5.40%	6.86%	5.14%	6.76%	5.93%	7.44%	6.14%	7.60%
	Gross Cycle Delta Heat Rate	kJ/kWh	base	-7	-367	-490	-417	-533	-427	-535	-409	-528	-468	-579	-482	-590

			Cycle													
	Parameter Description	Units	1	2	3	4	5	6	7	8	9	10	11	12	13	14
	BFP Power	kW	2696	2881	4977	4777	5288	5067	5730	5452	5620	5393	5970	5723	6481	6158
	Half-Net Cycle Efficiency	-	0.425	0.425	0.438	0.446	0.440	0.447	0.440	0.446	0.439	0.446	0.441	0.448	0.441	0.448
I	Salt Inlet Temperature	°C	565.5	565.5	566	600	566	600	566	600	566	600	566	600	566	600
J	Salt Return Temp	°C	310.5	323.9	300.4	299.5	314	314.3	330.4	331.3	299	297.1	312.5	312	329.3	329.2
K	Salt Flow Rate	kg/s	993.4	1046.6	910.7	788.4	952.9	823.5	1015.4	873.8	899.3	778	940.5	811.9	1003.1	861.8

2.5 Trade Studies

The impacts of final feedwater temperature, main steam pressure, feedwater pumping parasitics (half-net cycle efficiency), and salt return temperature were studied to determine the impact of key parameters on the cycle efficiency of the power block.

2.5.1 Impact of Final Feedwater Temperature

As can be seen in Table 2, the highest power block efficiency was demonstrated for cycle 12 and cycle 14 for main steam pressure of 260 bar-a (3770 psia), inlet steam and reheat steam temperature of 580°C (1076°F), and final feedwater temperature between 290°C (554°F) and 320°C (608°F). However, the efficiency improvement going from 290°C (554°F) to 320°C (608°F) is minimal as the required steam turbine extraction pressure gets close to the main steam pressure. Figure 6 shows the impact of final feedwater temperature on cycle efficiency for different inlet pressures and temperatures.

The impact of the increase in final feedwater temperature on efficiency gradually diminishes at temperatures above 290°C. This diminishing effect is more prominent at lower main steam pressure due to the lower boiling water temperature. Therefore, the optimum final feedwater temperature for a high-pressure cycle should be in the range of 290 to 300°C.

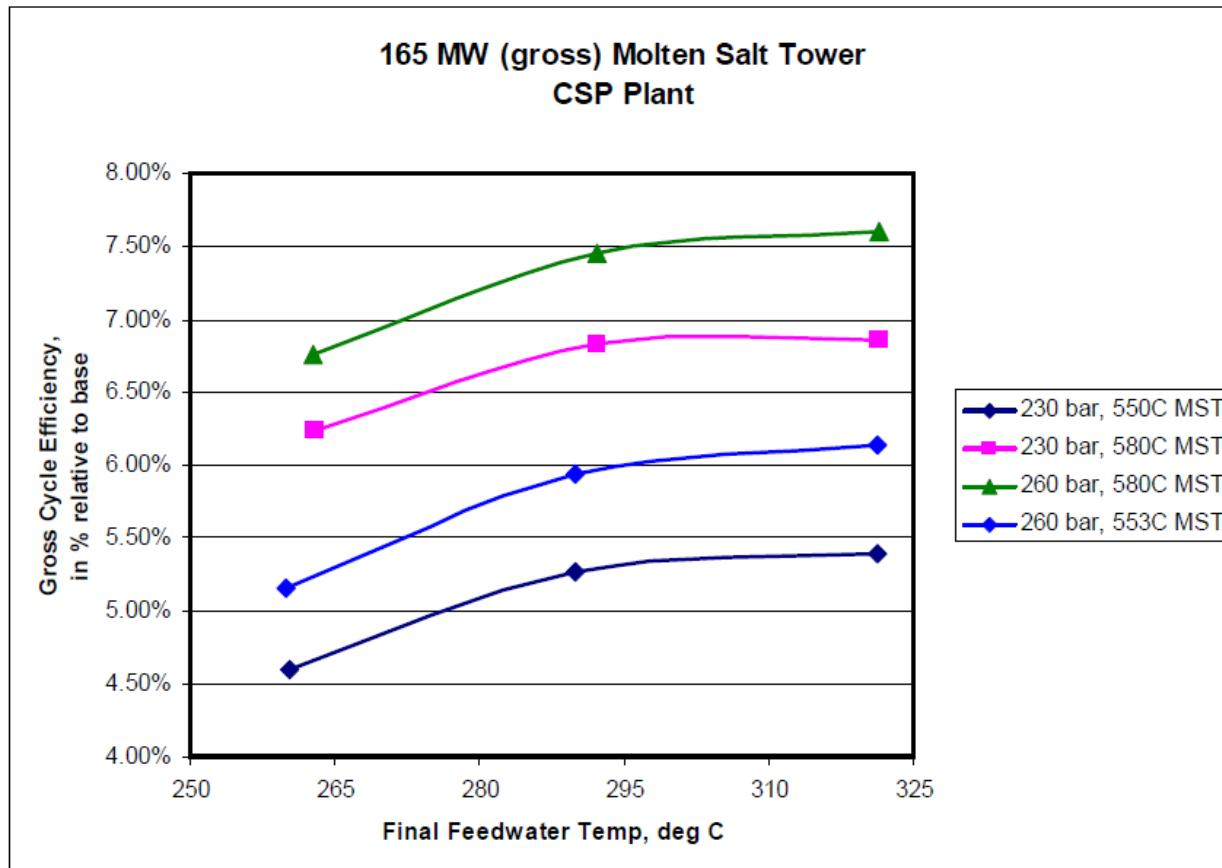


Figure 6. Impact of final feedwater temperature on power block efficiency

2.5.2 Impact of Main Steam Pressure

Figure 7 shows the impact of main steam pressure on cycle efficiency at main steam temperature (MST) of 553°C (1027°F) and final feedwater temperature of 260°C (500°F) and 290°C (554°F). The impact starts to diminish as the main steam pressure begins to exceed 230 bar-a (3335 psia).

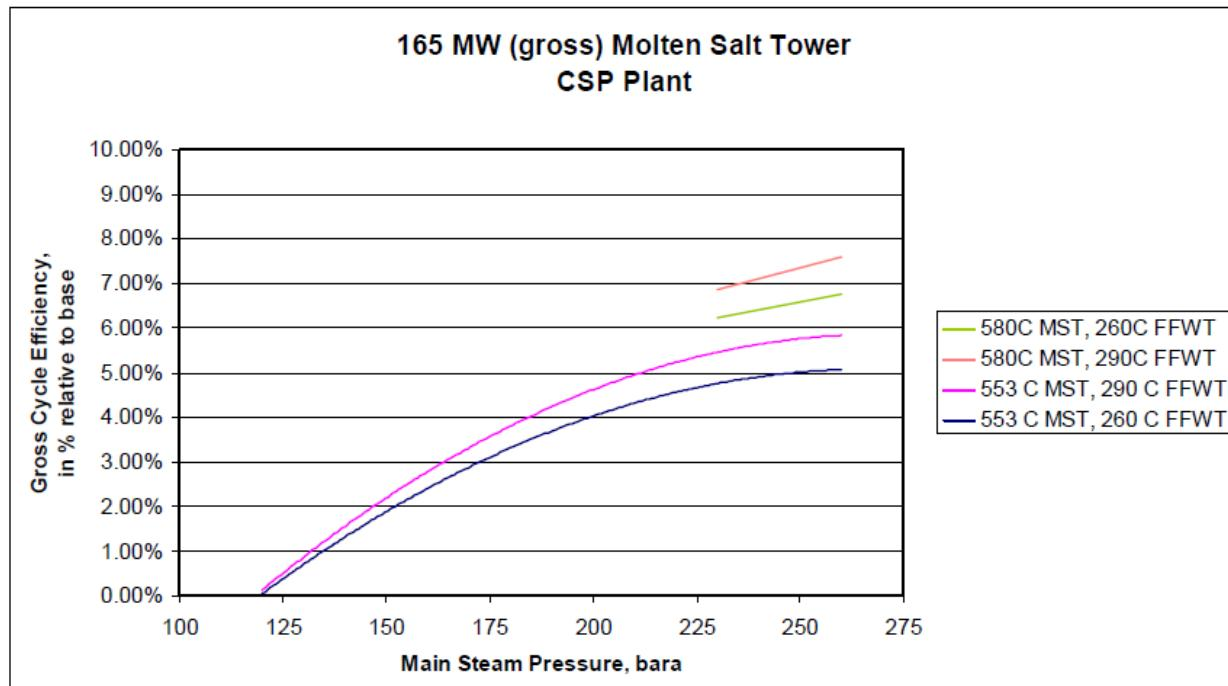


Figure 7. Impact of main steam pressure on power block gross efficiency

Figure 7 shows that with a steam temperature of 553°C (1022°F), a main steam pressure above 250 bar-a (3625 psi) does not increase the efficiency. With a higher steam temperature, the improvement in efficiency with higher pressure is still significant. It is also noteworthy that the increased final feedwater temperature (FFWT) gives a higher efficiency benefit at supercritical main steam pressure.

2.5.3 Half-net Cycle Efficiency

To fully evaluate the impact of different cycle parameters, the auxiliary power consumption of a boiler feed pump that increases with the main steam pressure must be included in the calculation. Therefore, the “half-net efficiency” accounts for the energy used to increase pressure of the feedwater from condenser pressure to feedwater pressure.

At a steam temperature of 553°C (1027°F), an increase in main steam pressure above 230 bar-a (3335 psia) does not provide incremental benefit in efficiency when the auxiliary power consumption is included (not plotted here). For this steam temperature, it is recommended that the main steam pressure for this power block be in the range of 200 to 230 bar-a (2900 psia to 3335 psia).

A higher steam temperature of 580°C (1076°F) pushes the efficiency maximum to higher steam pressure and justifies a main steam pressure of 260 bar-a (3770 psia) (see Figure 8). However, for economic reasons and operational aspects like startup time, a main steam pressure of 234 bar-a (3400 psia) and a steam temperature of 580°C (1076°F) at the steam turbine valves seems to be a reasonable compromise between performance, cost, and operational aspects of a CSP power block.

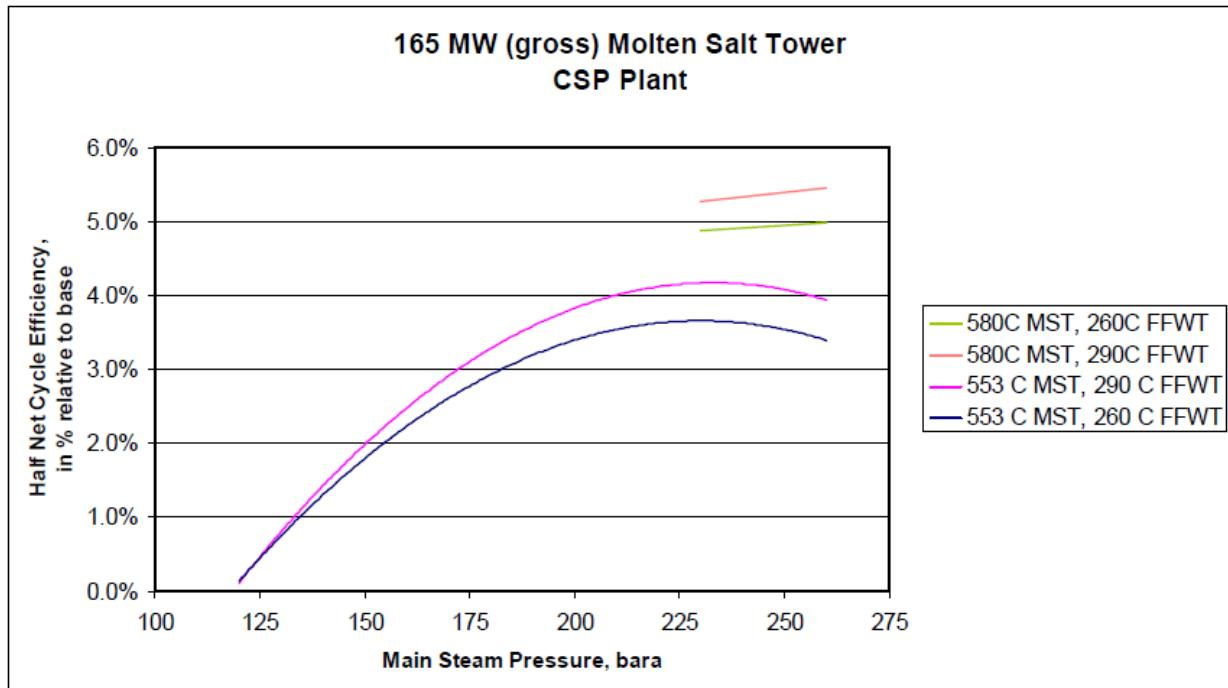


Figure 8. Impact of main steam pressure on half-net cycle efficiency

2.5.4 Salt Return Temperature

Molten-salt CSP power tower receivers are currently designed for the salt temperature rise from 290°C (554°F) cold salt inlet to 565°C (1050°F) hot salt outlet. These temperatures are associated with the current baseline power block design that uses main steam pressure of 120 bar-a (1740 psia) and returns cold molten salt from the steam generator at 290°C (554°F). However, changes in parameters such as the main steam pressure lead to a different salt return temperature as demonstrated in Table 2. The steam generator design used for calculation of Table 2 uses an aggressive pinch point of 5 K, resulting in a large economizer (preheater) surface. A revised receiver design to accommodate the changes in the parameters would be required in order to find the right balance between receiver surface area and boiler surface as a function of salt return temperature. A reasonable salt return temperature for a supercritical power block is expected to be in the range of 321 to 332°C (610 to 630°F).

2.6 Impacts on Receiver, Thermal Storage System, and Power Block Costs

The supercritical cycles studied here impact the cost of the receiver, thermal storage system, and power block relative to the baseline plant design due to changes in hot salt or cold salt temperatures and power block pressures and temperatures.

In the receiver, increasing the hot salt outlet temperature to 600°C from 565°C increases the thermal loss from 30 kW/m² to ~36 kW/m² [3]. This has a slight effect (~1%) on performance of

the receiver. Changing the salt temperature rise across the receiver relative to the baseline impacts the cold salt pumping parasitic because to maintain the same absorbed power, the mass flow rate must change inversely proportional to the temperature rise. The cold salt pump parasitic power is shown in Table 3 for selected systems. An additional cycle (Subcritical Baseline) has been defined that represents the baseline subcritical molten-salt systems studied previously. The advanced subcritical baseline cycle (based on Siemens' latest SST-900 subcritical steam turbine) outperforms the subcritical baseline cycle because the steam turbine in the advanced baseline has a higher isentropic efficiency in the intermediate pressure stages relative to the baseline subcritical steam turbine. This results in a gross cycle efficiency of the advanced subcritical turbine, which is more than 5% higher relative to the standard subcritical steam turbine.

Table 3. Cold and hot salt pump parasitic power consumption for selected cycles

	Cold Salt Temp, °C	Hot Salt Temp, °C	Cold Salt Pump			Hot Salt Pump		
			Mass Flowrate kg/s	Power, MW	kW/(kg/s)	Mass Flowrate kg/s	Power, MW	kW/(kg/s)
Subcritical Baseline	296	565	2454	12.1	4.93	984	1.04	1.055
Advanced Baseline Subcritical Cycle 1	310.5	565.5	2594	13.0	5.03	991	1.05	1.055
Supercritical Cycle 3	300.4	566	2487	12.3	4.95	908	0.96	1.055
Supercritical Cycle 4	299.5	600	2205	10.5	4.78	793	0.84	1.055
Supercritical Cycle 5	314	566	2626	13.3	5.05	952	1.01	1.055
Supercritical Cycle 6	314.3	600	2324	11.3	4.85	830	0.88	1.055
Supercritical Cycle 8	331.3	600	2444	12.0	4.92	873	0.92	1.055

The thermal storage system cost is impacted by the temperature difference between the hot and cold tanks, which affects the mass of salt required, and the temperature, which impacts the strength of the material. For a fixed thermal storage capacity, the mass of salt required is inversely proportional to the temperature differential. If the temperature difference between the hot and cold tank decreases relative to the baseline, then the mass of salt required increases to maintain the same capacity. Another factor that affects the cost of the thermal storage system is the temperature. Operating the hot salt tank at 600°C versus 565°C will require the hot tank shell to increase in thickness to make up for the reduction in the allowable strength of Type 347H stainless steel. In addition, the piping may need to be made from a higher strength alloy, such as a nickel-based alloy. But the increased costs of the nickel-based alloy in the hot piping is minor relative to the thermal storage system cost. Table 4 summarizes the impact of these changes on the specific costs of the thermal storage system for selected cycles.

Table 4. Thermal storage system specific costs for selected cycles

System	Hot Salt Temp, °C	Cold Salt Temp, °C	Nominal Salt Cost \$/kWh(t)	Nominal Tank Cost \$/kWh(t)	Total TSS Cost \$/kWh(t)
Subcritical Baseline	565	296	15.6	10.4	26
Advanced Baseline Subcritical Cycle 1	565.5	310.5	16.5	11.0	27.4
Supercritical Cycle 3	566	300.4	15.8	10.5	26.3
Supercritical Cycle 4	600	299.5	14.0	9.8	23.7
Supercritical Cycle 5	566	314	17.3	11.6	28.9
Supercritical Cycle 6	600	314.3	14.7	10.3	24.9
Supercritical Cycle 8	600	331.3	15.6	10.9	26.5

The power block costs of a supercritical plant are impacted by the cost of high-pressure systems in the water cycle. The components primarily affected are the steam turbine, steam generator, main steam piping system, high-pressure preheaters and feedwater piping, and boiler feedwater pumps. Due to the better efficiency relative to the baseline system, the heat rejection system can be designed smaller, which in the case of an Air Cooled Condenser may substantially reduce cost. A very rough estimate of the differential costs of an advanced baseline CSP subcritical power block and a supercritical power block operating at 234 bar-a, main steam and reheat steam of 580°C/580°C, final feedwater temperature of 290°C, is in the range of \$8 to 10 million.

2.7 Solar Plant Annual Performance and Levelized Cost of Energy

To fully understand the benefits and costs of supercritical power tower plants relative to the subcritical baselines, annual simulations and LCOE must be calculated. The System Advisory Model (SAM) was used to evaluate the cycles. The climate data used was Typical Meteorological Year 2 (TMY2) for Daggett, California, with an annual direct normal insolation of 2791 kWh/m². The plant configurations evaluated for the annual performance and LCOE are described in Table 5. These consist of the baseline configurations and supercritical steam plants that operate at hot salt temperatures of 565 and 600°C.

Table 5. Plant configurations evaluated for annual performance

Parameter	Baseline Sub-critical	Adv. Sub-critical Baseline Cycle 1	Super-critical Cycle 3	Super-critical Cycle 4	Super-critical Cycle 5	Super-critical Cycle 6	Super-critical Cycle 8
Gross Turbine Output, MW	165	165	165	165	165	165	165
Main Steam Pressure, bar-a	120	120	230	230	230	230	230
Main/Reheat Steam Temperature, °C	553	553	553	580	553	580	580
Cold Reheat Temperature, °C	370.7	370.7	285.1	303.2	284.8	302.9	303
Final Feedwater Temperature, °C	261	260.8	260.3	262.9	290	292.1	321.5

Parameter	Baseline Sub-critical	Adv. Sub-critical Baseline Cycle 1	Super-critical Cycle 3	Super-critical Cycle 4	Super-critical Cycle 5	Super-critical Cycle 6	Super-critical Cycle 8
Hot Salt Temperature, °C	565	565.5	566	600	566	600	600
Cold Salt Return Temperature, °C	296	310.5	300.4	299.5	314	314.3	331.3
Reheat Steam Pressure, bar-a	32.2	32.2	32.2	32.2	32.2	32.2	32.2
ACC Back Pressure, bar-a	0.155	0.152	0.152	0.152	0.152	0.152	0.152
Steam Generator Thermal Duty, MW (thermal)	401	382	365.1	359	362.8	357	357
Gross Cycle Efficiency, %	41.1	43.2	45.2	45.9	45.5	46.2	46.2
Boiler Feed Pump Power, kW	3175	2696	4977	4777	5288	5067	5452
Condensate Pump, kW	140	133	127	125	126	124	124
Cooling Fans, kW	2955	2811	2687	2646	2669	2629	2630
Auxiliaries, kW	700	700	700	700	700	700	700
Cold Pump Power, kW	12096	13038	12314	10534	13264	11263	12029
Hot Pump Power, kW	1009	1046	958	837	952	876	922
Heliostat Field Size, m ²	1962417	1962417	1962417	1962417	1962417	1962417	1962417
Receiver Rating, MW (thermal)	1000	1000	1000	1000	1000	1000	1000
Storage size (MWh)	5000	5000	5000	5000	5000	5000	5000

The financial assumptions used in the SAM analyses are listed in Table 6. The tax credit assumptions are a 10% federal investment tax credit, which reduces the federal and state depreciation basis. There are no investment-, capacity-, or production-based incentives assumed in the analysis.

The annual performance assumes 0% annual degradation and 90% availability. The plant should be able to maintain its nominal annual performance with a good operation and maintenance program.

Table 6. Financial assumption used in annual simulations

General	
Analysis Period	30 years
Inflation Rate	2.50%
Real Discount Rate	8.20%
Taxes and Insurance	
Federal Tax	35%/year
State Tax	8%/year
Sales Tax	7.75%
Insurance	0.50%
Salvage Value	
Net Salvage Value	0.0%
Property Tax	
Assessed Percent	100% of installed cost
Assessed Value Decline	0.0%

Property Tax	0.50%
Construction Period	Overnight
Load Parameters	
Loan Term	20 years
Load Rate	8%
Debt Fraction	54%
Solution Mode	Specify IRR Target
Minimum Required IRR	14%
PPA Escalation Rate	1.2%
Minimum Required DSCR	1.4
Require a positive cashflow	
Federal Depreciation	5-yr MACRS
State Depreciation	5-yr MACRS

The tower system costs are listed in Table 7. The power-block- specific costs for the supercritical plants include the additional costs of the supercritical steam turbine and once-through steam generator. These add approximately \$61/kWe to the power block cost. The heliostat field and receiver and tower characteristics are shown in Table 8 and Table 9 respectively. The power cycle and thermal storage parameters are listed in Table 10 and Table 11 respectively. Table 12 and Table 13 contain the plant parasitic power parameters. Some of these were extrapolated from [3].

Table 7. Tower system costs

Direct Capital Costs	
Site Improvement	\$20/m ²
Heliostat Field	\$120/m ²
Balance of Plant	\$250/kWe
Power Block	\$800/kWe (baseline), \$861/kWe (sc-steam)
Fossil Backup	\$0/kWt
Fixed Solar Field Cost	\$0.0
Fixed Tower Cost	\$1,927,000
Tower Cost Scaling Exponent	0.0113
Receiver Reference Cost	\$ 114,548,372
Receiver Reference Area	1967 m ²
Receiver Cost Scaling Factor	0.7
Contingency	0%
Indirect Capital Costs	
EPC and Owner Cost	\$0/acre, 15.5% of Direct Cost, \$0/Wac, \$0 fixed costs
Total Land Costs	\$10,000/acre, 0% of Direct Cost, \$0/Wac, \$0 fixed costs
Sales Tax applies to	80% of Direct Costs
Operation and Maintenance Costs	
Fixed Annual Cost	\$0.0/yr, 0% Escalation Rate
Fixed Cost by Capacity	\$50.00/kW-yr, 0% Escalation Rate
Variable Cost by Generation	\$3.00/MWh, 0% Escalation Rate
Fossil Fuel Cost	\$0.0/MMBtu, 0% Escalation Rate

Table 8. Heliostat field

Heliostat Properties	
Heliostat Width	9.7468 m
Heliostat Height	9.7468 m
Ratio of Reflective Area to Profile	1
Mirror Reflectance and Soiling	0.893
Heliostat Availability	0.99
Image Error	0.00153 rad
Heliostat Stow Deploy Angle	8 deg
Wind Stow Speed	17.9 m/s
Solar Field Layout Constraints	
Max Heliostat Distance to Tower Height Ratio	7.5
Min Heliostat Distance to Tower Height Ratio	0.75
Mirror Washing	
Water Usage per Wash	0.7L/m ² , aperture
Washes per Year	63
Land Area	
Non-Solar Field Land Area	45 acres
Solar Field Land Area Multiplier	1.3

Table 9. Tower and receiver characteristics

External Receiver	
Receiver Height	31.11 m
Receiver Diameter	19.44 m
Number of Panels	16
Coating Emittance	0.88
Recirculation Heater Efficiency	1
Materials and Flow	
HTF Type	Salt (60% NaNO ₃ 40% KNO ₃)
Material Type	Stainless AISI316 No other materials are available in SAM
Flow Pattern	1
Design Operation	
Solar Multiple	Varies with cycle
Min Receiver turndown fraction	0.16
Max receiver operation fraction	1.2
Receiver startup delay time	0.75 hr
Receiver startup delay energy fraction	0.25
Receiver Thermodynamic Characteristics	
Tube OD	80 mm
Tube Wall Thickness	1.25 mm
Required HTF Outlet Temperature	Varies with cycle (see Table 5, Table 1)
Max Temp to Receiver	Varies with cycle (see Table 5, Table 1)
Coating Absorptance	0.94
Heat Loss Factor	1
Max Receiver Flux	1000 kW/m ²
Tower Dimensions	
	275 m

Table 10. Power cycle parameters

Plant Capacity	
Design Turbine Gross Output	165 MWe
Estimated Gross to Net Conversion Factor	Varies with cycle (see Table 5)
Estimated Net Output at Design	Varies with cycle (see Table 5)
Power Block Design Point	
Rated Cycle Conversion Efficiency	Varies with cycle (see Table 5)
Design HTF Inlet Temp	Varies with cycle (see Table 5)
Design HTF Outlet Temp	Varies with cycle (see Table 5)
Boiler Operating Pressure	Varies with cycle (see Table 5)
Fossil Backup Boiler LHV efficiency	0.9
Steam cycle blowdown fraction	0.02 (subcritical only)
Plant Control	
Min Required Temp for Startup	500°C
Low-resource Standby Period	5 hours
Fraction of Thermal Power Needed for Standby	0.2
Power Block Startup Time	0.65 hours
Fraction of Thermal Power Needed for Startup	0.1
Min Turbine Operation	0.3
Max Turbine Over Design Operation	1.05
Turbine Inlet Pressure Control	Fixed Pressure
Cooling System	
Condenser Type	Air-cooled
Ambient Temperature at Design	43°C
ITD at Design Point	14°C
Condenser Pressure Ratio	1.0028
Min condenser pressure	2 in Hg
Cooling system part load levels	2

Table 11. Thermal storage parameters

Storage System	
Storage Type	Two Tank
Full Load Hours of TES	Varies with cycle, based on 5000 MWh energy
Tank Height	20.9 m
Tank Fluid Min Height	1 m
Parallel Tank Pairs	1
Wetted Loss Coefficient	0.4 W/m ² -K
Dry Loss Coefficient	0.25 W/m ² -K
Fossil Dispatch Mode	Minimum backup level
Initial Hot HTF Temp	Varies with cycle (see Table 5)
Initial Cold HTF Temp	Varies with cycle (see Table 5)
Initial Hot HTF Percent	30%
Cold Tank Heater Temp Set-Point	270°C
Cold Tank Heater Capacity	0.5 MWe
Hot Tank Heater Temp Set-Point	450°C
Hot Tank Heater Capacity	1 MWe
Tank Heater Efficiency	0.99
Thermal Storage Dispatch Control	
Uniform Dispatch	

Table 12. Parasitics parameters

Parasitic Energy Consumption	
Startup Energy of a Single Heliostat	0.0124 kWhe
Tracking Power for a Single Heliostat	0.0496 kWhe
Receiver HTF Pump Efficiency	0.8
Fraction of rated gross power consumed all times	0.005036 MWe/MWe
Required pumping power for HTF through power block	1.055 kJ/kg
Required pumping power for HTF through storage	0 kJ/kg
Piping Loss Coefficient	334 Wt/m
Piping Length Constant	0 m
Piping Length Multiplier	2.6
Balance of plant parasitic	See Table 13
Aux Heater, Boiler parasitic	0 MWe/MWcap

Table 13. Balance of plant parasitic parameters

	Baseline Sub- critical	Advanced Sub- critical Cycle 1	Super- critical Cycle 3	Super- critical Cycle 4	Super- critical Cycle 5	Super- critical Cycle 6	Super- critical Cycle 8
Boiler Feed Pump Power, kW	3175	2696	4977	4777	5288	5067	5452
Condensate Pump, kW	140	133	127	125	126	124	124
Cooling Fans, kW	2955	2811	2687	2646	2669	2629	2630
BOP Parasitics, MW	6.27	5.64	7.79	7.55	8.08	7.82	8.21
Balance of Plant Parasitic, MWe/MWcap	0.0385	0.0346	0.0478	0.0463	0.0496	0.0480	0.0503
bop_par_f=	1.00	1.00	1.00	1.00	1.00	1.00	1.00
bop_par_0=	0.1921	0.1921	0.1921	0.1921	0.1921	0.1921	0.1921
bop_par_1=	0.6644	0.6644	0.6644	0.6644	0.6644	0.6644	0.6644
bop_par_2=	0.1315	0.1315	0.1315	0.1315	0.1315	0.1315	0.1315

Finally, after the inputs from the tables were entered into SAM, the annual energy production and LCOE were calculated, as shown in Table 14. As can be seen, all the supercritical steam cycles listed in the table yielded more annual energy than the subcritical steam cycles. The highest performing supercritical steam cycle (Cycle 5) outperformed the subcritical baseline by 13.5%. The supercritical cycles that operated with a hot salt temperature of 600°C (cycles 4, 6, and 8) had slightly lower annual energy productions than the supercritical cycle operating at 566°C hot salt temperature.

When all effects on costs are included, the LCOEs for all the supercritical steam cycles plants are less than the baseline subcritical steam plant by 7 to 10%. Also, the advanced baseline plant (Cycle 1) has an LCOE that is about 3.8% higher than the LCOE of the lowest cost supercritical cycle plant (Cycle 6), but more than 7% less than the baseline subcritical plant. The supercritical cycle plants 3 and 6 have nearly the same LCOE but operate at different molten-salt temperatures (565 and 600°C, respectively). Because their costs are so close, other factors may drive the ultimate selection of a configuration, such as margin on the receiver design, fatigue of the thermal storage tank, margin on the stability of the nitrate salt, or risk tolerance of the investor.

Table 14. Summary of annual energy production and leveled cost of energy

Parameter	Baseline Sub-critical	Advanced Sub-critical Cycle 1	Super-critical Cycle 3	Super-critical Cycle 4	Super-critical Cycle 5	Super-critical Cycle 6	Super-critical Cycle 8
Annual Energy Produced, GWh	721	785	817	802	818	813	791
Annual Energy Delta, %	0.0	8.9	13.3	11.2	13.5	12.8	9.7
LCOE, Real, cents/kWh	11.2	10.4	10.0	10.1	10.2	10.0	10.4
LCOE delta, %	0.0	-7.2	-10.4	-10.0	-9.2	-10.6	-7.3
Plant Capacity Factor, %	57.2	62.4	65.6	63.4	66.2	64.7	63.5

Intentionally left blank.

3. CONCLUSIONS

In this study, 14 different subcritical and supercritical steam cycles were examined to determine the effects of main steam pressure and temperature, final feedwater temperature, and salt return temperature on the gross and half-net efficiency. The annual power production and LCOE on the most promising subcritical and supercritical cycles were calculated using SAM. The supercritical steam cycle plants produced more annual energy than the subcritical steam cycle plants. Two supercritical plants had the lowest LCOE relative to the other cycles. Both operated at 230 bar-a main steam pressure: one was designed for 600°C hot salt and 292°C final feedwater temperature (Cycle 6), the other was designed for 565°C hot salt and a lower final feedwater temperature of 260°C (Cycle 3). Based on these results, it appears economically and technically feasible to incorporate supercritical steam turbines into molten-salt power towers.

Intentionally left blank.

4. REFERENCES

- [1] J.E. Pacheco. *Final Test and Evaluation Results from the Solar Two Project*, SAND2002-0120, Sandia National Laboratories, Albuquerque, NM, 2002
- [2] U.S. Department of Energy. SunShot Vision Study, February 2012,
<http://www1.eere.energy.gov/solar/pdfs/47927.pdf>
- [3] G.J. Kolb. *An Evaluation of Possible Next-Generation High Temperature Molten-Salt Power Towers*, SAND2011-9320, Sandia National Laboratories, Albuquerque, NM, 2011
- [4] G.J. Kolb, C.K. Ho, T.R. Mancini, J.A. Gary. *Power Tower Technology Roadmap and Cost Reduction Plan*, SAND2011-2419, Sandia National Laboratories, Albuquerque, NM, 2011.

Distribution

External (electronic)

Ranga Pitchumani, Ranga.Pitchumani@EE.Doe.Gov
US DOE Office of the Solar Energy Technology Program
Route Symbol: EE-2A
Building: L'ENF950
Washington, DC 20585

Joseph Stekli, joseph.stekli@ee.doe.gov
US DOE Office of the Solar Energy Technology Program
Route Symbol: EE-2A
Building: L'ENF950
Washington, DC 20585

Mark Mehos, Mark.Mehos@nrel.gov
National Renewable Energy Laboratory
15013 Denver West Parkway
Golden, CO 80401

Max Peters, peter@research.ge.com
GE Global Research
1 Research Circle ES-106
Niskayuna, NY 12309

John Van Scoter, jvs@esolar.com
eSolar
3355 W. Empire Avenue
Suite 200
Burbank, CA 91504

Craig Tyner, craig@esolar.com
eSolar
3355 W. Empire Avenue
Suite 200
Burbank, CA 91504

Dale Rogers, dale@esolar.com
eSolar
3355 W. Empire Avenue
Suite 200
Burbank, CA 91504

Mike Slack, mike@esolar.com
eSolar
3355 W. Empire Avenue
Suite 200
Burbank, CA 91504

Andy Heap, Andrew@esolar.com
eSolar
3355 W. Empire Avenue
Suite 200
Burbank, CA 91504

David Gross, dgross@esolar.com
eSolar
3355 W. Empire Avenue
Suite 200
Burbank, CA 91504

Bruce Kelley, Bruce.Kelly@solar.abengoa.com
Abengoa Solar
11500 West 13th Avenue
Lakewood, CO

Hank Price, Hank.Price@solar.abengoa.com
Abengoa Solar
11500 West 13th Avenue
Lakewood, CO

Lorin Vant Hull, solarvanthull@aol.com
Professor of Physics Emeritus
128 N Red Bud Trail
Elgin, TX, 78621

Bob Bradshaw, rwbards@gmail.com
756 Mariposa Ave
Livermore, CA 94551-4242

Brian Iverson, bdiverson@byu.edu
Department of Mechanical Engineering
Brigham Young University
435 Crabtree Building
Provo, UT 84602

Greg Kolb, gikolb@mail.com

SolarReserve

1205 Lawrence Ct. NE
Albuquerque, NM 87112

David Wasyluk, dtwasyluk@babcock.com
Babcock & Wilcox Power Generation Group
20 S. Van Buren Avenue
Barberton, Ohio 44203

Thorsten Wolf, tnwolf@siemens.com
Siemens Energy, Inc,
Fossil Power Generation
4400 Alafaya Trail
MC Q2-386
Orlando, FL 32826

Nishant Muley, nishant.muley@siemens.com
Siemens Energy, Inc,
Fossil Power Generation
4400 Alafaya Trail
MC Q2-386
Orlando, FL 32826

Internal (electronic)

1	MS0721	Tatro, Marjorie	6100
1	MS0769	Moya, Ronald	6600
1	MS0762	Parks, Bradley	6630
1	MS0783	Monthan, Chad	6634
1	MS1033	Hanley, Charles	6112
1	MS1104	Torres, Juan	6120
1	MS1127	Shinde, Subhash	6123
1	MS1127	Andraka, Charles	6123
1	MS1127	Christian, Joshua	6123
1	MS1127	Ghanbari, Cheryl	6123
1	MS1127	Gill, David	6123
1	MS1127	Ho, Clifford	6123
1	MS1127	Kolb, William	6123
1	MS1127	Sment, Jeremy	6123
1	MS1127	Yellowhair, Julius	6123
1	MS0899	Technical Library	9536 (electronic copy)

